Inorganic Chemistry

Article

pubs.acs.org/IC

Structure and Properties of *fac*-$[Re^{I}(CO)_3(NTA)]^{2-}$ (NTA^{3-} = Trianion of Nitrilotriacetic Acid) and *fac*-$[Re^{I}(CO)_3(L)]^{n-}$ Analogues Useful for Assessing the Excellent Renal Clearance of the *fac*-$[^{99m}Tc^{I}(CO)_3(NTA)]^{2-}$ Diagnostic Renal Agent

Jeffrey Klenc,*[,†] Malgorzata Lipowska,[†] Pramuditha L. Abhayawardhana,[‡] Andrew T. Taylor,[†] and Luigi G. Marzilli*[,‡]

[†]Department of Radiology and Imaging Sciences, Emory University, Atlanta, Georgia 30322, United States

[‡]Department of Chemistry, Louisiana State University, Baton Rouge, Louisiana 70803, United States

Supporting Information

ABSTRACT: We previously identified two new agents based on the $[^{99m}Tc^{V}O]^{3+}$ core with renal clearances in human volunteers 30% higher than that of the widely used clinical tracer ^{99m}Tc-MAG_3 (MAG_3^{5-} = penta-anion of mercaptoacetyltriglycine). However, renal agents with even higher clearances are needed. More recently, we changed our focus from the $[^{99m}Tc^{V}O]^{3+}$ core to the discovery of superior tracers based on the *fac*-$[^{99m}Tc^{I}(CO)_3]^{+}$ core. Compared to ^{99m}Tc-MAG_3, *fac*-$[^{99m}Tc^{I}(CO)_3(NTA)]^{2-}$ (NTA^{3-} = trianion of nitrilotriacetic acid) holds great promise by virtue of its efficient renal clearance via tubular secretion and the absence of hepatobiliary elimination, even in patients with severely reduced renal function. We report here NMR, molecular (X-ray) structure, and solution data on *fac*-$[Re^{I}(CO)_3(NTA)]^{2-}$ with a $-CH_2CO_2^{-}$ dangling monoanionic chain and on two *fac*-$[Re^{I}(CO)_3(L)]^{-}$ analogues with either a $-CH_2CONH_2$ or a $-CH_2CH_2OH$ dangling neutral chain. In these three *fac*-$[Re^{I}(CO)_3(L)]^{n-}$ complexes, the *fac*-$[Re^{I}(CO)_3(N(CH_2CO_2)_2)]^{-}$ moiety is structurally similar and has similar electronic properties (as assessed by NMR data). In reported and ongoing studies, the two *fac*-$[^{99m}Tc^{I}(CO)_3(L)]^{-}$ analogues with these neutral dangling chains were found to have pharmacokinetic properties very similar to those of *fac*-$[^{99m}Tc^{I}(CO)_3(NTA)]^{2-}$. Therefore, we reach the unexpected conclusion that in *fac*-$[^{99m}Tc^{I}(CO)_3(L)]^{n-}$ agents, renal clearance is affected much more than anticipated by features of the core plus the chelate rings (the $[^{99m}Tc^{I}(CO)_3(N(CH_2CO_2)_2)]^{-}$ moiety) than by the presence of a negatively charged dangling carboxylate chain.

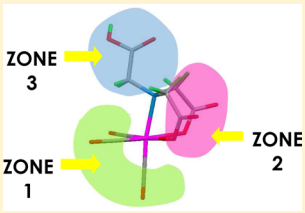

INTRODUCTION

^{99m}Tc radiopharmaceuticals are widely employed in nuclear medicine for imaging and for assessing physiological function and disease. The close relationship between Tc and Re chemistry has led to the use of the Re/^{99m}Tc strategy of synthesizing and characterizing Re complexes and performing animal biodistribution studies with the ^{99m}Tc analogues. Renal ^{99m}Tc radiopharmaceuticals are used to image the kidney, evaluate suspected renal disease, and monitor renal function. Image quality is dependent on rapid removal of the radiotracer from the circulating plasma by the kidney; the rate of removal provides an important measurement of renal function.[1] The rate-limiting factor for the removal of any substance by the kidney is the renal plasma flow, an important physiological parameter. This parameter could be measured indirectly with a nonmetabolized substance that is completely extracted with each circulation through the kidneys. The small aromatic compound, *p*-aminohippuric acid (PAH, Figure 1), approximates this ideal substance, and its clearance, termed the effective renal plasma flow (ERPF), has served as a benchmark for the indirect measurement of renal plasma flow.

A radiopharmaceutical related to PAH, ^{131}I-orthoiodohippuran (^{131}I-OIH, introduced in 1960, Figure 1),[2] was subsequently demonstrated to have a clearance highly correlated with PAH and an ^{131}I-OIH/PAH clearance ratio of 87%.[3] The development of ^{131}I-OIH was a major step forward. However, the relatively long half-life (8 days) and beta emission of ^{131}I raised the possibility of delivering a large radiation dose to patients with reduced renal function; moreover, the 364 keV gamma photon emitted by ^{131}I was too high in energy for an optimal imaging tracer. The limitations of ^{131}I stimulated the development of ^{99m}Tc-based tracers. ^{99m}Tc has a short half-life (6 h) and lacks beta emission, features that minimize the radiation dose to patients; in addition, ^{99m}Tc emits a 140 keV photon optimal for imaging. However, a coordination complex could not be a close structural analogue of PAH.

By the late 1980s, the best of several ^{99m}Tc tracers developed for imaging the kidneys and estimating ERPF was ^{99m}Tc-mercaptoacetyltriglycine (^{99m}Tc-MAG_3, Figure 1), although the clearance of ^{99m}Tc-MAG_3 was only 50−65% that of ^{131}I-OIH, making the tracer suboptimal for the estimation of ERPF.[4] Nevertheless, ^{99m}Tc-MAG_3 is now the most commonly used radiotracer for this purpose, even though the ^{99m}Tc-MAG_3

Received: March 13, 2015
Published: June 12, 2015

DOI: 10.1021/acs.inorgchem.5b00584
Inorg. Chem. 2015, 54, 6281−6290

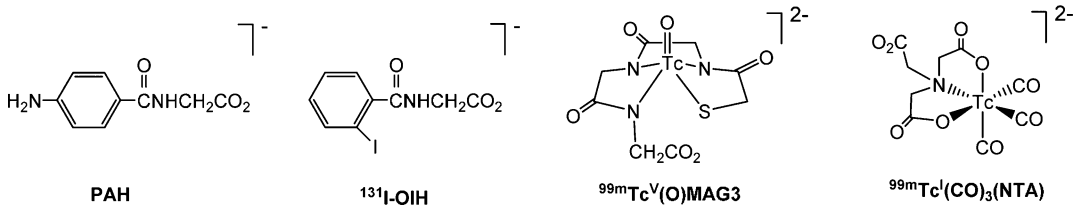

Figure 1. Structure and charge of agents used to evaluate effective renal plasma flow at physiological pH.

Scheme 1

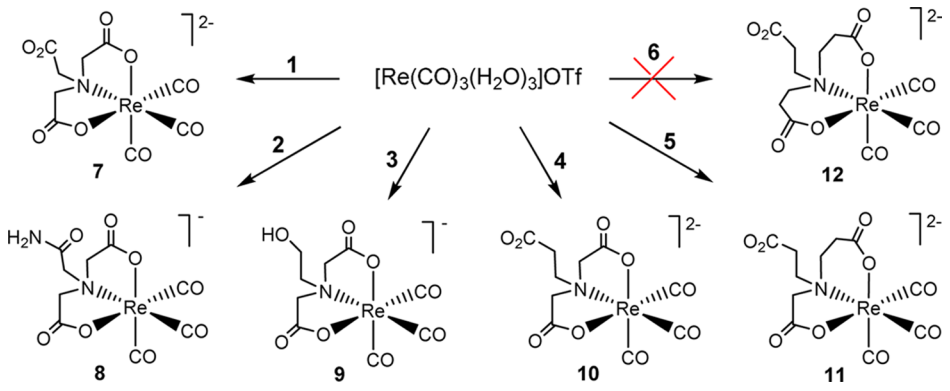

tracer is eliminated to a small extent via the hepatobiliary tract.[5] Furthermore, this undesirable hepatobiliary elimination of the ^{99m}Tc-MAG$_3$ tracer is exacerbated in patients with impaired renal function.[6−8]

Our group has focused on the development of a ^{99m}Tc tracer that exhibits a renal clearance closer to the ERPF physiological limit. ^{99m}Tc-MAG$_3$ has a $[^{99m}Tc^{V}O]^{3+}$ core.[9] In earlier work, we employed a strategy of designing new ligands (L), chemically characterizing new $Re^{V}O(L)$ complexes, and evaluating the biodistribution of $^{99m}Tc^{V}O(L)$ analogues.[10−12] The exploration of how changing L influenced $^{99m}Tc^{V}O(L)$ renal clearance[10−18] led to a better understanding of $M^{V}O(L)$ chemistry and biodistribution. These efforts successfully identified two agents, ^{99m}Tc-DD-EC (ECH$_6$ = ethylene dicysteine) and ^{99m}Tc-*syn*-D-MAEC (MAECH$_5$ = mercaptoacetamide ethylene cysteine), with clearances in humans 30% higher than that of ^{99m}Tc-MAG$_3$.[11,12] However, these $^{99m}Tc^{V}O(L)$ agents were not sufficiently superior to ^{99m}Tc-MAG$_3$ in human volunteers to justify patient clinical studies. The most successful ligands were tetradentate N_xS_y donors with dangling (not coordinated) carboxyl group(s), features also present in ^{99m}Tc-MAG$_3$.

More recently, we changed our focus from the $[^{99m}Tc^{V}O]^{3+}$ core to the discovery of superior tracers based on the *fac*-$[^{99m}Tc^{I}(CO)_3]^{+}$ core, but we retained the guiding principle that agents with superior clearance would likely have a carboxyl group, usually attached to a chelate ring atom or on a dangling chain terminating with the carboxyl group.[12,19−23] Tridentate ligands are among the best ligand types to use for preparing agents for the versatile *fac*-$[^{99m}Tc^{I}(CO)_3]^{+}$ core.[24−29] N_xO_y donor tridentate ligands can be used with this core.[22,30−32] In a relatively short time, we discovered that the *fac*-$[^{99m}Tc^{I}(CO)_3(NTA)]^{2-}$ tracer [referred to here as ^{99m}Tc-(CO)$_3$(NTA), prepared from nitrilotriacetic acid (NTAH$_3$, **1**)] holds promise as a successor to ^{99m}Tc-MAG$_3$.[22,33,34] ^{99m}Tc-(CO)$_3$(NTA) has a clearance rate comparable to that of ^{131}I-OIH in rats and humans and has no observed hepatobiliary excretion.[22,33,34] The putative structure of ^{99m}Tc(CO)$_3$(NTA) should differ significantly from those of PAH, ^{131}I-OIH, and even ^{99m}Tc-MAG$_3$ (Figure 1). Thus, for designing even better renal agents with the *fac*-$[^{99m}Tc^{I}(CO)_3]^{+}$ core, ^{99m}Tc-(CO)$_3$(NTA) serves as a new starting point for the Re/^{99m}Tc chemistry/biodistribution strategy that we employed successfully with the $[M^{V}O]^{3+}$ core.

In this work, we explore the chemistry of *fac*-$[Re^{I}(CO)_3(L)]^{n-}$ complexes in which L are close analogues of NTA, including some L expected to form complexes having a dangling chain with an uncoordinated carboxyl group, a feature that has been considered essential for tubular transport.[35] Each L has been evaluated by initial biological studies of *fac*-$[^{99m}Tc^{I}(CO)_3(L)]^{n-}$ complexes **7**−**10**.[36,37] We report the characterization of the *fac*-$[Re^{I}(CO)_3(NTA)]^{2-}$ complex in solution and as a salt that permitted crystallographic determination of its molecular structure. Extensive comparisons of NMR data, solid-state X-ray structures, and solution behavior of *fac*-$[Re^{I}(CO)_3(NTA)]^{2-}$ and its *fac*-$[Re^{I}(CO)_3(L)]^{n-}$ analogues reported here have provided valuable insights as to why *fac*-$[^{99m}Tc^{I}(CO)_3(NTA)]^{2-}$ exhibits the observed desirable pharmacokinetic properties. Because all of these new complexes exhibit facial geometry, we commonly omit the *fac*- designation when discussing specific new complexes, especially in solution.

EXPERIMENTAL SECTION

Materials. Nitrilotriacetic acid (NTAH$_3$, **1**, Aldrich), *N*-(2-acetamido)iminodiacetic acid (ADAH$_2$, **2**) and *N*-(2-hydroxyethyl)-iminodiacetic acid (HDAH$_2$, **3**, both from Acros Organics), and nitrilodiacetic-propionic acid (NDAPH$_3$, **4**, TCI America) were used as received. Nitrilodipropionic-acetic acid (NDPAH$_3$, **5**) was synthesized in similar yield and purity (confirmed by ^{1}H NMR methods) by the published method.[38] Nitrilotripropionic acid (NTPH$_3$, **6**, TCI America) was used as received.

General Procedures. An aqueous stock solution (0.1 M) of $[Re(CO)_3(H_2O)_3]OTf$ (prepared as previously reported[39]) was prepared and used as needed. The rhenium complexes were purified by gel filtration over Sephadex G-15 beads, eluting with deionized water at a rate of 0.5 mL/min. NMR spectra were recorded on Bruker 400 MHz spectrometers. Electrospray mass spectrometry (ESI-MS,

DOI: 10.1021/acs.inorgchem.5b00584
Inorg. Chem. 2015, 54, 6281−6290

negative mode) was performed on a Thermo Finnigan LTQ-FT instrument. HPLC analyses (monitored at 254 nm) were performed on a Waters Breeze system equipped with a Waters 2487 detector, Waters 1525 binary pump, and XTerra MS C18 column (5 μm; 4.6 × 250 mm). The HPLC gradient was composed of 0.05 M triethylammonium phosphate at pH 2.5 aqueous buffer (solvent A) and methanol (solvent B). The HPLC gradient started with 100% A from 0 to 3 min. The eluent switched at 3 min to 75% A/25% B, at 6 min to 66% A/34% B, and remained for 3 more min, followed by linear gradients of 66% A/34% B to 34% A/66% B from 9 to 20 min; and 34% A/66% B to 100% A from 20 to 30 min (flow rate of 1 mL/min).

Preparation of *fac*-[Re(CO)$_3$(L)]$^{n-}$. The product anionic complexes (**7**−**11**) formed in solution from ligands **1**−**5** are shown in Scheme 1. As explained in more detail below, we use the same numbers here as for the isolated salts, which typically have the dangling carboxyl group protonated. An aqueous solution of L (**1**−**5**; 0.5 mmol, 5 mL) was added to a stirred solution of *fac*-[Re(CO)$_3$(H$_2$O)$_3$]OTf (0.5 mmol, 5.0 mL) and neutralized with 1 M NaOH to maintain a pH near 6−7 throughout the reaction. A small aliquot of the reaction mixture was heated at 70 °C and monitored by HPLC until completion of the reaction; one sharp peak was observed for each complex [with RT values of 14 min (**7**), 10.5 min (**8**), 13.2 min (**9**), 13.8 min (**10**), and 14 min (**11**)]. For NTPH$_3$ (**6**), the reaction mixture was monitored for 24 h, but no peak indicating reaction progress was observed. The reaction mixture of **6** was also heated and monitored at pH 7.5 and pH 8.5, with the same negative results as those at pH 6−7.

After the aliquots were removed, the remainder of each reaction mixture (for ligands **1**−**5**) was kept at room temperature, and reaction progress was monitored by HPLC for 24 h. The reaction mixture was concentrated to 1 mL and purified by gel filtration. UV-active fractions were combined and concentrated under reduced pressure to yield *fac*-Re(CO)$_3$(L). Each sample was dried to yield a white powder; ^{1}H NMR spectra (pH 6) and HRMS data (Supporting Information) confirm that a salt with the expected *fac*-[Re(CO)$_3$(L)]$^{n-}$ product anion (**7**−**11**) was isolated.

Crystal Formation. Highly purified samples of complexes **8** and **9** were dissolved in a minimal amount of water, and diluted slightly with ethanol until the solution became faintly cloudy. Solutions kept at 4 °C for several days deposited X-ray quality crystals of Na[Re(CO)$_3$(ADA)]·2H$_2$O (**8**·2H$_2$O) and Na[Re(CO)$_3$(HDA)]·5H$_2$O (**9**·5H$_2$O). A small sample (powder) of **7** or **10** was dissolved in 2−3 mL of water, and solid NEt$_4$Cl (∼30 mg) was added. Each mixture was heated for 2−3 min to obtain a clear solution and was then left undisturbed. Very small amounts of X-ray quality crystals of NEt$_4$[Re(CO)$_3$(NTAH)] (**7**) and NEt$_4$[Re(CO)$_3$(NDAPH)]·2H$_2$O (**10**·2H$_2$O) formed over several days. Attempts to crystallize a salt of Re(CO)$_3$(NDPA) (**11**) by similar methods were unsuccessful, possibly because of its larger, more flexible, and less symmetrical structure.

Crystal Structure Determination. For complexes **7**−**10**, a suitable crystal was coated with Paratone N oil, suspended in a small fiber loop, and placed in a cooled nitrogen gas stream at 173 K (**7**, **8**, and **9**) or 110 K (**10**) on a Bruker D8 APEX II CCD sealed tube diffractometer with graphite monochromated Mo Kα (λ = 0.71073 Å, for complexes **8** and **9**) or Cu Kα (λ = 1.54178 Å, for complexes **7** and **10**) radiation. Data collection, indexing, and initial cell refinements were all carried out with APEX II software.[40] Frame integration and final cell refinements were conducted with SAINT software.[19]

Structures were solved by using direct methods and difference Fourier techniques (SHELXTL, V6.12).[41] Hydrogen atoms were placed in their expected chemical positions by using the HFIX command and were included in the final cycles of least-squares with isotropic U_{ij}'s related to the atoms ridden upon. All non-hydrogen atoms were refined anisotropically. Scattering factors and anomalous dispersion corrections were taken from the International Tables for X-ray Crystallography.[42] Compound **8** has four independent molecules in the asymmetric unit. The methylene groups of the tetraethylammonium cation are disordered over two positions with occupancies 0.746:0.254 in compound **10**. The tetraethylammonium cation is disordered over two almost equivalent positions in compound **7**. Structure solution, refinement, and generation of publication materials were performed by using SHELXL software;[41] graphics were prepared by using ORTEP-3 for Windows.[43]

RESULTS AND DISCUSSION

In Scheme 1, we illustrate the results obtained from treating *fac*-[Re(CO)$_3$(H$_2$O)$_3$]OTf,[39] the rhenium analogue of the *fac*-[^{99m}Tc(CO)$_3$(H$_2$O)$_3$]$^+$ labeling precursor,[27,44] with several aminopoly(carboxylic acid) ligands [NTAH$_3$ (**1**), ADAH$_2$ (**2**), HDAH$_2$ (**3**), NDAPH$_3$ (**4**), NDPAH$_3$ (**5**), and NTPH$_3$ (**6**)]. Ligands **1**−**5** formed complexes (**7**−**11**), with a metal-to-ligand ratio of 1:1 that was confirmed by analytical methods (see Supporting Information). However, NTPH$_3$ (**6**) did not form a *fac*-[Re(CO)$_3$(L)]$^{n-}$ product. This overall reaction pattern was observed in past studies in which ligands **1**−**5**, but not **6**, were labeled with *fac*-[^{99m}Tc(CO)$_3$(H$_2$O)$_3$]$^+$.[37] The structures illustrated in the Scheme are consistent with our previous research on *fac*-M(CO)$_3$(polyaminocarboxylate) complexes (M = Re and ^{99m}Tc),[32] demonstrating that the coordination of amine groups is preferred over the carboxyl groups at physiological pH. The structures are also consistent with several previous solution studies on the relative ability of ligands **1** and **4**−**6** to form chelate complexes with various metal cations.[45−48] [Note: In Scheme 1 and throughout the text, we use the same number for the complex in solution or in the solid state. However, the isolated solids have the dangling carboxyl group protonated. For example, we use **7** to refer to the solid as NEt$_4$[*fac*-Re(CO)$_3$(NTAH)], but we refer to the solution species more simply as Re(CO)$_3$(NTA). Because the charge on **7** in solution depends on pH, we do not specify its charge.]

Time courses of the reaction mixtures of ligands **1**−**6** with *fac*-[Re(CO)$_3$(H$_2$O)$_3$]$^+$ at pH 6−7 were monitored by HPLC at 20 °C (Supporting Information) and at 70 °C. For ligands **1**−**5**, reactions were complete within 30 min at 70 °C and showed one major HPLC peak corresponding to well-defined *fac*-[Re(CO)$_3$(L)]$^{n-}$ complexes (**7**−**11**). Ligands having an iminodiacetic moiety (**1**−**4**) formed complexes (**7**−**10**) that have a plane of symmetry. For **5**, however, the product has one 5-membered and one 6-membered chelate ring (Scheme 1), and the single product HPLC peak contains a pair of enantiomers of **11**. The HPLC profiles of complexes **7**−**11** were very similar to those of their ^{99m}Tc(CO)$_3$ analogues.[36,37] In contrast, NTPH$_3$ (**6**), which can form only 6-membered chelate rings, did not form detectable amounts of product even after prolonged heating at pH 6−7. Because one can assume that the N in NTPH$_3$ (with three attached propionate groups) would be more basic than the N in NTAH$_3$ (with three attached acetate groups), we evaluated **6** at a higher pH but still found the same negative result (no detectable product). Ligand **5**, like **6**, has three carboxyl groups, but **5** can form one 5-membered chelate ring. Ligand coordination is thus sufficiently favored by the ability to form one 5-membered chelate ring, producing adequately robust *fac*-[^{99m}Tc(CO)$_3$(L)]$^{n-}$ agents. Even though **5** has three carboxyl groups, **2** and **3** (with two carboxyl groups) form complexes more quickly than **5**. Thus, the formation of the iminodiacetic tridentate chelate with two five-membered rings appears to be very favorable for facilitating the formation of the tracer complexes.

X-ray Crystallography. The molecular structures of the anions in complexes **7**−**10** are shown in Figure 2, and the

DOI: 10.1021/acs.inorgchem.5b00584
Inorg. Chem. 2015, 54, 6281−6290

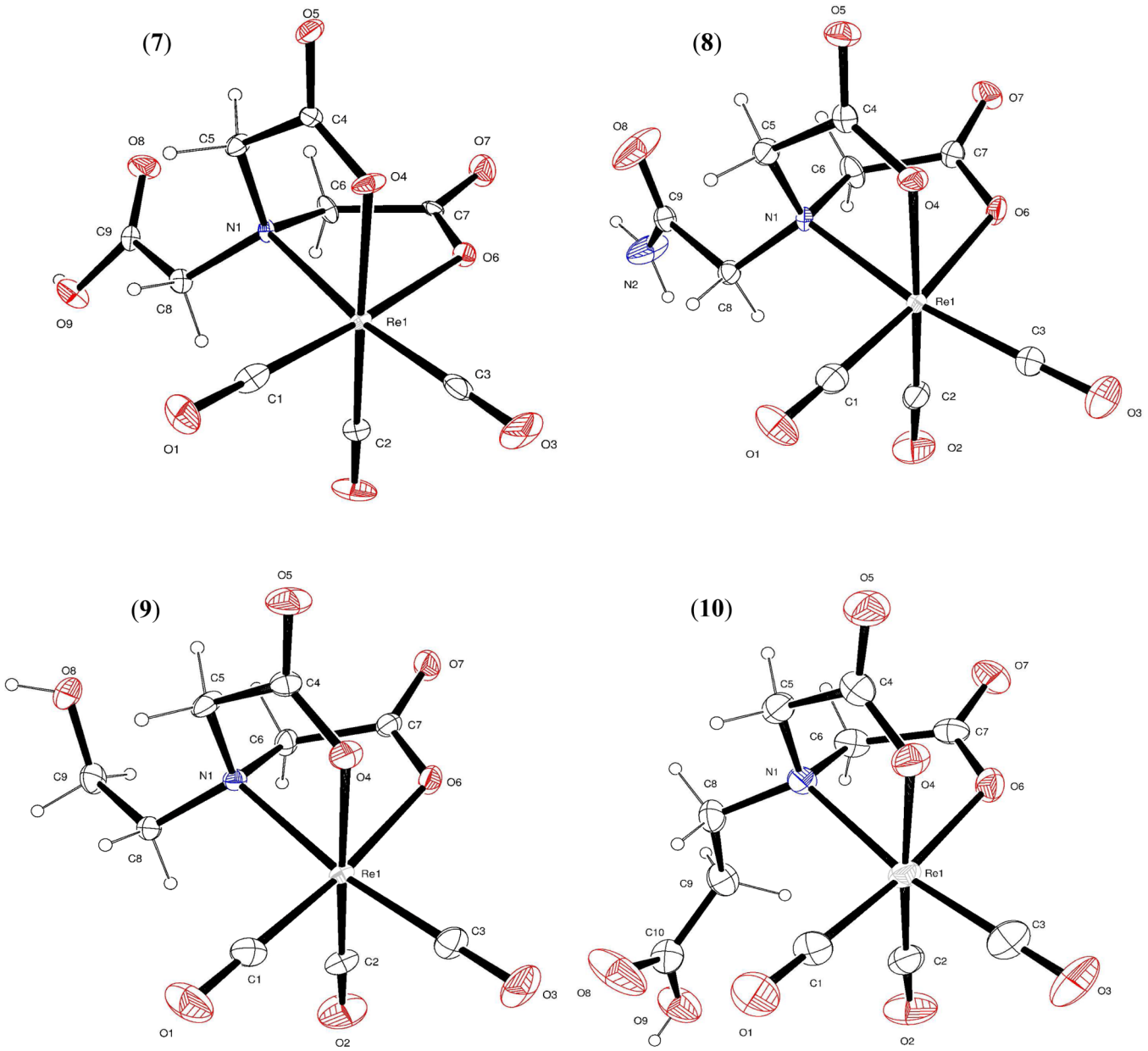

Figure 2. ORTEP plots of the anions in NEt_4[*fac*-$Re(CO)_3$(NTAH)] (**7**), Na[*fac*-$Re(CO)_3$(ADA)]·$2H_2O$ (**8**·$2H_2O$), Na[*fac*-$Re(CO)_3$(HDA)]·$5H_2O$ (**9**·$5H_2O$), and NEt_4[*fac*-$Re(CO)_3$(NDAPH)]·$2H_2O$ (**10**·$2H_2O$). The thermal ellipsoids are drawn with 50% probability.

crystal data and details of structural refinement for these complexes are summarized in Table 1. The crystal structure of NEt_4[*fac*-$Re(CO)_3$(NTAH)] (**7**) confirmed an ONO coordination mode with two adjacent 5-membered chelate rings. Complexes formed between $NTAH_3$ and various metal ions, including Re and Tc, have been investigated previously;[22,48,49] however, no crystallographically determined molecular structures of Re or Tc complexes with this ligand have been reported.

Complexes **8**, **9**, and **10** each have an ONO coordination mode with a net negatively charged inner metal-coordination-sphere core, as does **7**. The bond distances and angles of complexes **8**−**10** are also strikingly similar to those of **7**, as expected (Table 2). The Re−N or Re−O bonds of ∼2.2 Å are characteristically long for complexes with *fac*-$[Re^{I}(CO)_3]^+$ compared to the typically shorter bond lengths of ∼2.0 Å from these donor atoms to other metals or even to higher-valent Re.[50,51] We have noted previously that the typical nonbonded distances between 5-membered ring donor atoms are independent of such differences in M−(donor atom) bond lengths.[52] The longer Re^{I}−(donor atom) bond lengths, combined with the characteristic similarity in nonbonded separation of chelate ring donor atoms, result in the following patterns of bond angles: acute N−Re^{I}−N or N−Re^{I}−O chelate ring bite angles (much less than 90°), and C−Re^{I}−N or C−Re^{I}−O bond angles involving carbonyl carbons that are clearly less than 180° for trans angles and greater than 90° for orthogonal angles.[52,53] Bond angles in complexes **7** to **10** are consistent with these trends (Table 2). In addition, the dangling group extends in a practically identical manner in complexes **7**, **8**, and **9**, but the orientation of the dangling chain is very different in **10** (Figure 2). This comparison indicates that the position of the uncoordinated dangling group may be largely independent of interactions between the chain and the

DOI: 10.1021/acs.inorgchem.5b00584
Inorg. Chem. 2015, 54, 6281−6290

Table 1. Crystal Data and Structure Refinement for NEt_4[*fac*-$Re(CO)_3$(NTAH)] (7), Na[*fac*- $Re(CO)_3$(ADA)]·$2H_2O$ (8·$2H_2O$), Na[*fac*-$Re(CO)_3$(HDA)]·$5H_2O$ (9·$5H_2O$), and NEt_4[*fac*-$Re(CO)_3$(NDAPH)]·$2H_2O$ (10·$2H_2O$)

	7	8·$2H_2O$	9·$5H_2O$	10·$2H_2O$
empirical formula	$C_{17}H_{27}N_2O_9Re$	$C_9H_{12}N_2NaO_{10}Re$	$C_9H_{19}N_1NaO_{13}Re$	$C_{18}H_{33}N_2O_{11}Re$
fw	589.6	517.4	558.44	639.66
λ (Å)	1.54178	0.71073	0.71073	1.54178
crystal system	monoclinic	triclinic	triclinic	monoclinic
space group	$P2_1/n$	$P\bar{1}$	$P\bar{1}$	$P2_1$
a (Å)	7.6992 (9)	13.002 (4)	7.066 (2)	9.4535 (5)
b (Å)	10.5716 (11)	15.807 (5)	8.141 (3)	10.0859 (5)
c (Å)	25.726 (3)	17.133 (7)	16.647 (7)	12.7840 (7)
α (deg)	90	68.511 (6)	99.428 (6)	90
β (deg)	96.931 (4)	68.084 (4)	97.203 (6)	92.8469 (15)
γ (deg)	90	78.604 (4)	109.912 (4)	90
V (Å^3)	2078.6 (4)	3032.2 (18)	871.1 (5)	1217.41 (11)
T (K)	173	173	173	110
Z	4	8	2	2
ρ calc (mg/m^3)	1.884	2.267	2.129	1.745
abs coeff (mm^{-1})	11.9	8.1	7.066	10.27
$2\theta_{max}$ (deg)	68.2	26.4	29.8	68.1
$R\ [I > 2\sigma(I)]^a$	0.037	0.024	0.026	0.016
wR^{2b}	0.097	0.058	0.067	0.040
data/param	3585/328	12396/892	4891/226	3823/347
res. dens (eÅ^{-3})	2.21, −1.27	1.58, −0.99	2.59, −2.00	0.80, −0.69
Flack parameter				0.046(5)

$^aR = (\sum||F_o| - |F_c||)/\sum|F_o|$. $^bwR^2 = [\sum[w(F_o^2 - F_c^2)^2]/\sum[w(F_o^2)^2]]^{1/2}$, in which $w = 1/[\sigma^2(F_o^2) + (dP)^2 + (eP)]$ and $P = (F_o^2 + 2F_c^2)/3$.

Table 2. Selected Bond Distances (Å) and Bond Angles (deg) for NEt_4[*fac*-$Re(CO)_3$(NTAH)] (7), Na[*fac*-$Re(CO)_3$(ADA)]·$2H_2O$ (8·$2H_2O$), Na[*fac*-$Re(CO)_3$(HDA)]·$5H_2O$ (9·$5H_2O$), and NEt_4[*fac*-$Re(CO)_3$(NDAPH)]·$2H_2O$ (10·$2H_2O$)

	7	8·$2H_2O$	9·$5H_2O$	10·$2H_2O$
Re−N(1)	2.266(5)	2.257(3)	2.246(3)	2.253(3)
Re−O(4)	2.124(4)	2.140(3)	2.123(3)	2.123(4)
Re−O(6)	2.111(4)	2.135(3)	2.141(3)	2.138(4)
Re−C(1)	1.920(7)	1.912(4)	1.910(4)	1.924(6)
Re−C(2)	1.908(6)	1.901(4)	1.909(4)	1.898(7)
Re−C(3)	1.913(7)	1.918(4)	1.914(4)	1.907(4)
O(4)−Re−C(1)	98.1(2)	94.83(14)	96.54(15)	95.9(2)
O(4)−Re−C(2)	173.7(2)	173.89(13)	173.57(14)	174.3(3)
O(4)−Re−C(3)	96.1(2)	96.22(14)	94.69(15)	92.7(2)
O(4)−Re−N(1)	77.16(16)	77.46(10)	78.68(11)	78.07(16)
O(4)−Re−O(6)	79.93(17)	78.40(11)	78.15(12)	79.05(18)
O(6)−Re−C(1)	175.9(2)	172.72(13)	173.57(14)	173.4(3)
O(6)−Re−C(2)	94.7(2)	97.49(14)	95.91(15)	95.2(3)
O(6)−Re−C(3)	96.4(2)	95.22(14)	96.32(14)	97.0(3)
O(6)−Re−N(1)	78.10(16)	77.65(10)	77.05(11)	76.8(2)
N(1)−Re−C(1)	98.0(2)	98.4(2)	98.5(2)	98.1(2)
N(1)−Re−C(2)	98.7(2)	97.3(2)	97.7(2)	100.3(2)
N(1)−Re−C(3)	171.9(2)	171.2(2)	171.4(2)	169.6(2)
C(6)−N(1)−C(5)	111.2(5)	109.4(3)	110.0(3)	108.9(3)
C(8)−N(1)−Re	110.3(4)	113.4(2)	112.7(2)	117.9(2)

$[Re(CO)_3(N(CH_2CO_2)_2)]^-$ inner coordination sphere. Rather, packing forces may dictate the orientation of the longer chain in **10**, where several angles that involve the N atom anchoring the dangling chain differ significantly from the corresponding angles in **7**, **8**, and **9** (Table 2). However, the chelate ring appears to be less sensitive to these effects, as evident from the very similar bond angles [e.g., C(6)−N(1)−C(5)] in each chelate ring of the four structurally characterized complexes.

In summary, crystallography confirms that the structures of **7**−**10** are consistent with previous reports;[31,54,55] the inner coordination sphere structures of **8** and **9** do not differ from that of **7** and are not influenced by the nature of the dangling chains. Because attempts to crystallize **11** were not successful, comparisons between **7** and **11** must rely on the NMR and solution studies described below.

NMR Spectroscopy. Bond lengths and angles are sometimes insensitive to changes in electron richness within the chelate rings, but ^{13}C NMR chemical shift data can provide useful insight concerning both electron richness and structure. Complexes **7**−**11** were characterized by ^1H and ^{13}C NMR

DOI: 10.1021/acs.inorgchem.5b00584
Inorg. Chem. 2015, 54, 6281−6290

spectroscopy in D_2O; selected data appear in Table 3, and complete data are listed in Supporting Information). Table 4

Table 3. ^1H and ^{13}C NMR Shifts (ppm) of the 5-Membered Chelate Rings in Complexes 7−11 (15 mM in D_2O, 25 °C) at Near Neutral pH[a]

	7	8	9	10	11
signal/(pH)	(8.40)	(7.23)	(7.45)	(7.74)	(7.50)
		^1H NMR Shifts			
$-N-CH_2$ *exo*-CH	4.06	4.04	4.03	3.91	3.85
$-N-CH_2$ *endo*-CH	3.95	3.98	3.76	3.62	3.71
		^{13}C NMR Shifts			
$-N-CH_2$	66.21	66.29	65.89	65.06	64.03
$-CO_2^-$	186.80	186.10	186.20	186.05	186.27

[a] The pH values are in parentheses at the top of the columns.

Table 4. ^1H and ^{13}C NMR Shifts (ppm) of $Re(CO)_3$(NTA) (7), $Re(CO)_3$(NDAP) (10), and $Re(CO)_3$(NDPA) (11) (15 mM in D_2O, 25 °C) at High and Low pH[a]

	7		10		11	
signal/(pH)	(8.40)	(2.46)	(7.74)	(2.16)	(7.50)	(2.47)
			^1H NMR Shifts			
$-N-CH_2$ dangling	4.08	4.27	3.70	3.75	3.74	3.78
$-C-CH_2$ dangling			2.63	2.86	2.62	2.87
					2.55	2.79
			^{13}C NMR Shifts			
$-N-CH_2$ dangling	73.35	70.99	69.01	67.00	65.08	63.17
$-C-CH_2$ dangling			36.21	32.95	35.39	32.14

[a]Values are in parentheses at the top of columns).

lists ^1H and ^{13}C NMR shifts at high (~7.5−8.5) and low (~2.0−2.5) pH values for 15 mM solutions of **7**, **10**, and **11** in D_2O. The ^1H and ^{13}C NMR shifts for complexes **8** and **9** were not significantly altered when the pH was changed from high (~7.5−8.5) to low (~2.0−2.5) pH (cf. Tables S1 and S2 in Supporting Information).

NMR signals were assigned by analyzing the splitting pattern, integration, and data from 2D NMR experiments. Following our previous convention for *fac*-$[Re(CO)_3L]^n$ complexes,[52,56] we designate the magnetically distinct ring CH_2 protons in **7** as *endo*-H or *exo*-H, according to their orientation either toward (*endo*) or away (*exo*) from the carbonyl ligands (Figure 3). The most extensive studies were performed on $Re(CO)_3$(NTA) (**7**), both because it is the analogue of the promising ^{99m}Tc renal agent and because it is a prototype for assigning signals for **8**, **9**, and **10**. $Re(CO)_3$(NDPA) (**11**) was also studied extensively because its chemical behavior under strongly acidic and basic conditions is quite different from that of **7**. To explain these differences, we also conducted detailed NMR experiments to assign signals for **11**.

^1H and ^{13}C NMR Assignments for $Re(CO)_3$(NTA) (7). The ^1H NMR spectrum of **7** at pH 8.40 (Supporting Information) shows a singlet integrating to two protons and an AB pattern; the two AB "doublets" each integrated to two protons. The two equivalent 5-membered chelate rings in **7** create a magnetically equivalent environment for the protons of the dangling $-CH_2CO_2^-$ moiety, thus allowing the unambiguous assignment of the singlet at 4.08 ppm to that moiety. The singlet for the dangling $-CH_2CO_2H$ group moved downfield as the pH of the solution was lowered (Table 4). A plot of the chemical shift of this singlet versus pH shows a typical sigmoid curve (Figure 4). Chemical shift changes observed for other

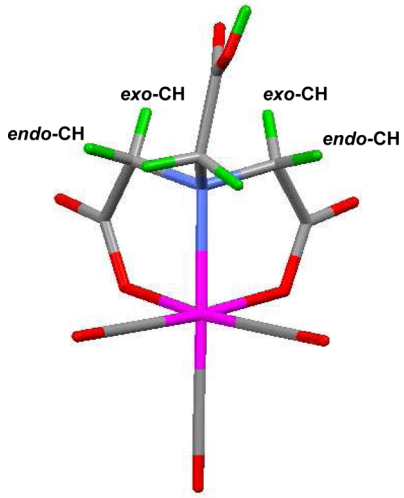

Figure 3. Anion of NEt_4[*fac*-$Re(CO)_3$(NTAH)] (**7**) showing the designation of *endo*- and *exo*-CH protons of the methylene group in the 5-membered chelate rings.

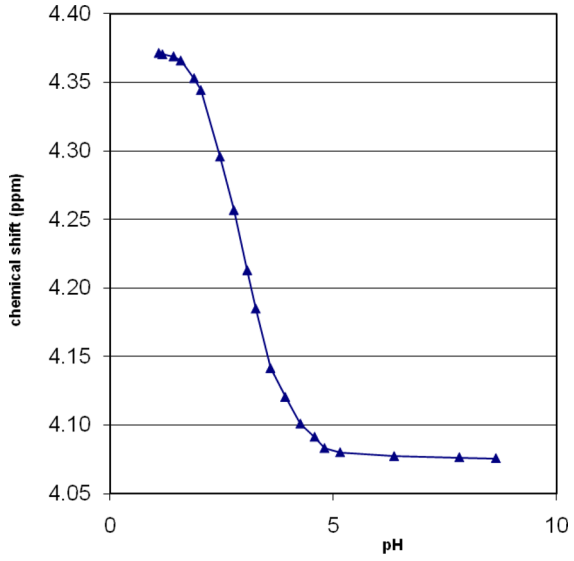

Figure 4. Variation with pH of the chemical shift (ppm) of the ^1H NMR signal arising from the dangling CH_2 group of $Re(CO)_3$(NTA) (**7**) (15 mM) in D_2O at 25 °C.

peaks were insignificant. This singlet for **7** has an HSQC cross-peak to a ^{13}C NMR signal at 73.35 ppm, thus assigning it to the CH_2 group of the dangling $-CH_2CO_2^-$ moiety. Furthermore, the HSQC cross-peaks from the two AB "doublets" to a ^{13}C NMR signal at 66.21 ppm allow the assignment of the signals to the equivalent methylene groups in the chelate rings.

In the ROESY spectrum for **7** (at pH ~2.5, Supporting Information), the CH_2 singlet (4.27 ppm) of the dangling $-CH_2CO_2H$ chain has strong and weak NOE cross-peaks, respectively, to the 3.96 and 4.03 ppm signals of the AB doublets arising from the $-CH_2CO_2^-$ protons of the chelate rings. The shorter average nonbonded distances from the

DOI: 10.1021/acs.inorgchem.5b00584
Inorg. Chem. 2015, 54, 6281−6290

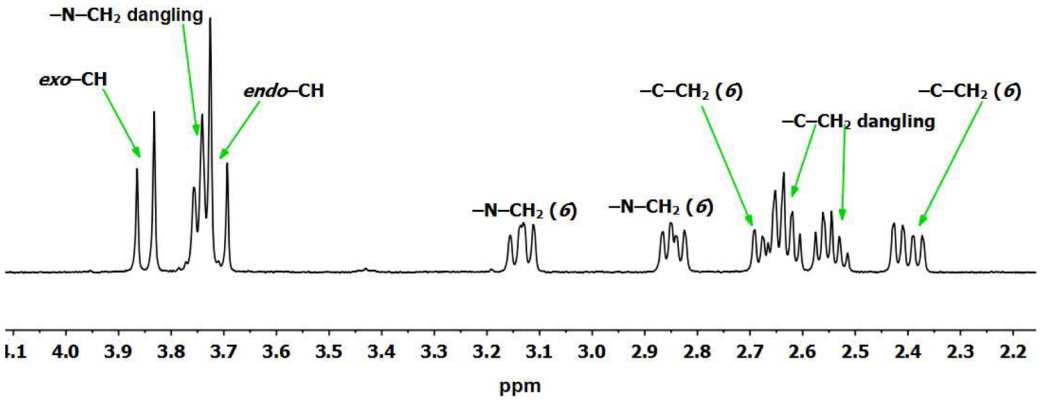

Figure 5. ^{1}H NMR spectrum of Re(CO)$_3$(NDPA) (**11**) in D$_2$O (pH 7.50) at 25 °C. The *exo*-CH and *endo*-CH signals of the 5-membered chelate ring are labeled. The (6) label denotes CH multiplets from the 6-membered ring.

dangling group protons to the *endo*-CH protons (2.29 Å) than to the *exo*-CH protons (3.26 Å) assigns the 3.96 and 4.03 ppm AB doublets to the *endo*-CH and *exo*-CH protons, respectively.

^{1}H and ^{13}C NMR Assignments for Re(CO)$_3$(ADA) (8), Re(CO)$_3$(HDA) (9), and Re(CO)$_3$(NDAP) (10). After the pH was lowered to 2, the shifts of the ^{1}H and ^{13}C NMR signals of **8** and **9** showed no significant change, as expected (Supporting Information). However, the two multiplets of the methylene groups of the dangling $-CH_2CH_2CO_2^-$ moiety of **10** clearly shifted downfield, with the expected protonation of the carboxyl group at pH 2.16 (Table 4). The greater shift change for the upfield multiplet (~0.24 ppm) than for the downfield multiplet (~0.05 ppm) allowed the assignment of the upfield multiplet (~2.63 ppm at pH ~7.5) to the $-CH_2CO_2^-$ group, and the downfield multiplet (~3.70 ppm at pH ~7.5) to the N$-CH_2$ group of the dangling $-CH_2CH_2CO_2^-$ moiety. The ^{13}C NMR signals of these methylene groups were assigned from HSQC spectra at the two different pH values (Supporting Information).

^{1}H and ^{13}C NMR Assignments for Re(CO)$_3$(NDPA) (11). In the spectrum of **11** at pH 7.50 (Figure 5), the clear AB ^{1}H NMR doublet at 3.85 ppm and the AB doublet at 3.71 ppm (overlapped with a multiplet) have an HSQC cross-peak with the ^{13}C NMR signal at 64.03 ppm. These AB doublets have COSY cross-peaks (strong) only with each other. Consequently, these signals can all be unambiguously assigned to the methylene group of the 5-membered chelate ring. All other CH ^{1}H NMR signals arise from the two CH_2CH_2 moieties, and these assignments, as well as other ^{13}C NMR assignments are described and summarized in Supporting Information.

Ligand Challenge Reactions and the Effect of Acid and Base on Re(CO)$_3$(NTA) (7) and Re(CO)$_3$(NDPA) (11). The ^{1}H NMR signals of **7** in D$_2$O (15 mM, pH 8.40) showed no change, even after several weeks. After the pH of this solution of **7** was lowered to 2.46, no changes were observed in the ^{1}H NMR spectrum even after 14 days. Challenge reactions were carried out on solutions of **7** (5 mM) in D$_2$O by adding a 5-fold molar ratio of potentially coordinating ligands. Moderately basic ligands [histidine, cysteine, or 4-methylimidazole, giving respective pH values of 8.2, 7.4, and 9.2] and highly basic ligands [isopropylamine, diethylenetriamine (dien), and dimethylaminopyridine, in solutions at pH 7] did not alter the ^{1}H NMR signals for **7** even after 2 weeks.

A 5 mM solution of **11** in D$_2$O (pH 7.59) was stable for two months. When a 5-fold molar ratio of histidine was added to this solution, the pH of the solution changed to ~7.9, but no changes were observed in the ^{1}H NMR signals for **11** after 2 weeks. The spectrum of another solution of **11** in D$_2$O (15 mM) was recorded at pH 7.50 and then at pH 2.47. Some ^{1}H NMR signals had shifted in the first spectrum recorded (at 15 min) for the pH 2.47 solution (Supporting Information). Very small ^{1}H NMR signals corresponding to the free NDPAH$_3$ ligand were also observed at 15 min. These signals gradually grew with time. At 10 days, the intensity of the signals indicated that ~26% of **11** decomposed to form free NDPAH$_3$.

Without pH control, addition of the three highly basic ligands with **7** and of dien with **11** increased the solution pH to ~11–12. The original methylene signals for the five-membered chelate rings for both **7** and **11** decreased owing to the H to D exchange, consistent with the slight acidity of such methylene protons.[57] Spectral changes occurred more rapidly with **7** than with **11**. The ^{1}H NMR spectra for **7** in all three cases showed very similar peaks for an unidentified decomposition product, suggesting that these changes were caused by the high basicity of the solutions and not by any direct effect of the basic amines on **7**. Adding a 5-fold molar ratio of sodium hydroxide to **11** (5 mM) in D$_2$O increased the pH of the solution to ~12.5. After 1 day, the 5-membered chelate ring methylene ^{1}H NMR signals for **11** were detectable as a result of the H to D exchange and decomposition. When the pH was lowered, the signals indicating decomposition were identified as being from free NDPAH$_3$. Both observations (slower H to D exchange and longer decomposition times for **11** than for **7**) are indicative of a more electron-rich metal center in **11** than in **7**. In summary, Re(CO)$_3$(NDPA) (**11**) is robust under neutral conditions but decomposes under strongly acidic or highly basic conditions. In contrast, Re(CO)$_3$(NTA) (**7**) decomposes under strongly basic conditions about twice as fast as **11** but is robust from highly acidic to slightly basic conditions.

Relationship of the Acid and Base Sensitivity of 7 and 11 to Structure and to the Electronic Nature of the Chelate Rings. To explore other possible reasons for these differences in the effects of acid and base on complexes **7** and **11**, we compared the shifts of the corresponding N$-CH_2$ ^{13}C NMR signals of the dangling group and the 5-membered chelate rings of these complexes (Tables 3 and 4).

For pH conditions at which the dangling group is monoanionic (~7.5–8.5), the N$-CH_2$ ^{13}C NMR signal of the dangling moiety is 8.27 ppm more upfield for **11** than for **7**. Also, the N$-CH_2$ ^{13}C NMR signal of the 5-membered chelate

DOI: 10.1021/acs.inorgchem.5b00584
Inorg. Chem. 2015, 54, 6281–6290

ring in **11** is 2.18 ppm more upfield than that for **7**. This upfield shift indicates that the Re^{I} center is more electron rich in **11** than in **7**, and therefore, the CH_2 group of the 5-membered chelate ring of **11** is less prone to deprotonation by base at high pH than are the CH_2 groups in the 5-membered rings of **7**. This finding is consistent with the H to D exchange just mentioned above because deprotonation of the methylene group is the first step in the H to D exchange process.[57] However, the electron richness of the Re^{I} center of **11** will make the carboxyl end of the six-membered ring more prone to dissociation. We expect that an undetectably low amount of the ring-opened form of **11** exists. At low pH, protonation of the dissociated carboxyl group should increase the abundance of this undetectable open form, and the greater abundance would lead to the eventual dissociation of more donor groups and to the release of the free $NDPAH_3$ ligand, explaining the observation of the $NDPAH_3$ signals in low pH solutions of **11**. When complex **7** was treated with acid, no changes in the ^{1}H NMR signals of **7** were observed, nor were $NTAH_3$ signals observed. This robustness of **7** toward acid undoubtedly arises from two of its properties: the Re^{I} center is less electron rich in **7** than in **11**, and both chelate rings in **7** are favorable 5-membered chelate rings. Both of these properties of **7** reduce the amount of chelate ring opening that leads to decomposition.

Relationship of Structure, Charge, and the Electronic Nature of the Chelate Rings to Biodistribution. The atoms of *fac*-$[M^{I}(CO)_3(L)]^{n-}$ anions that are most likely to influence biodistribution are those exposed to the solvent and thus accessible for interactions with proteins and receptors. These atoms can be grouped into three zones (Figure 6). The three facially coordinated carbonyl ligands constitute ZONE 1. This "constant" zone is very similar for all complexes and thus will not be a significant source of the observed variation in biodistribution as the chelate ligand is changed. ZONE 2 consists of the CH_2CO_2 or $CH_2CH_2CO_2$ components of the chelate rings, except for the $N-CH_2$ *endo*-CH protons. ZONE 3 consists of the "variable" dangling chain and the *endo*-CH protons of the chelate ring $N-CH_2$ groups. To evaluate the relative influence of ZONE 2 and ZONE 3 on biodistribution, we begin by assessing the electronic nature of ZONE 2 in **7**, **8**, and **9**; these complexes have very similar structures, differing only in the dangling chain (Figure 2).

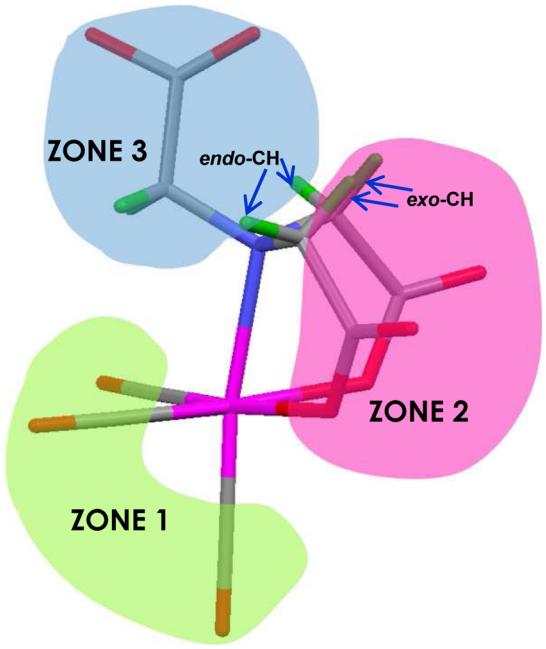

Figure 6. Side view of $Re(CO)_3(NTA)$ (**7**), showing the "constant" ZONE 1 (green), the "solvent-exposed chelate ring" ZONE 2 (rose), and the "variable dangling-chain" ZONE 3 (blue). The figure shows the location of the *exo*-CH protons in ZONE 2 and the *endo*-CH protons in ZONE 3.

A dangling chain could influence the NMR shifts of a proton by such factors as a through-space anisotropic effect, an alteration of the solvation sphere, or a through-bond inductive effect. Only the latter factor is likely to influence the shifts of atoms that are spatially remote from the dangling chain. The 5-membered-ring *exo*-CH protons and carbon atoms are relatively far from the dangling chain; thus, the shifts of the NMR signals of these atoms should be sensitive to only through-bond inductive effects. The shifts of the *exo*-CH ^{1}H NMR signals of complexes **7**, **8**, and **9** are very similar (Table 3), as are the shifts of the 5-membered ring ^{13}C NMR signals (Table 4). Thus, although **7** has a dinegative charge and **8** and **9** are mononegative, both types of ZONE 2 signals (the *exo*-CH ^{1}H NMR and chelate ring ^{13}C NMR signals) indicate that ZONE 2 has very similar electronic properties in **7**, **8**, and **9**. The dangling chains in these complexes appear to affect the electronic properties of the $[Re(CO)_3(N(CH_2CO_2)_2)]^{-}$ moiety in a very similar manner. However, the ^{13}C NMR data for $Re(CO)_3(NDAP)$ (**10**) are consistent with a small but clear effect of the $-CH_2CH_2CO_2^{-}$ dangling chain on the electronic properties of this moiety.

ZONE 3 differs, of course, in the nature of the dangling chain of **7**, **8**, and **9**. The *endo*-CH protons are in ZONE 3 and are positioned close to the dangling chain. As expected from this proximity, the ^{1}H NMR shift of the *endo*-CH signal for **9** does differ from those of the *endo*-CH signal for **7** and **8**, which are quite similar to each other (Table 3).

Despite lacking a negatively charged pendant carboxyl group and having a low monoanionic charge, the ^{99m}Tc analogues of **8** and **9**, $^{99m}Tc^{I}(CO)_3(ADA)$ and $^{99m}Tc^{I}(CO)_3(HDA)$, each exhibit a rapid renal extraction rate, practically identical to that of $^{99m}Tc(CO)_3(NTA)$.[36] Therefore, the negative charge of the dangling acetate group of $^{99m}Tc(CO)_3(NTA)$ (the ^{99m}Tc analogue of **7**) has no identifiable effect on the renal extraction of that agent via the tubules. Furthermore, the many points of similarity in the structures and the electronic properties of ZONE 2 of the $[Re(CO)_3(N(CH_2CO_2)_2)]^{-}$ moiety in complexes **7**, **8**, and **9** lead us to conclude that the primary factor responsible for the favorable pharmacokinetic properties of their ^{99m}Tc analogues resides chiefly within ZONE 2 of the $[^{99m}Tc^{I}(CO)_3(N(CH_2CO_2)_2)]^{-}$ moiety and much less so in the dangling group. In previous studies of ^{99m}Tc renal agents spanning decades, an uncoordinated negative carboxyl group (often in a dangling chain) appeared to be the key factor favoring a high rate of renal extraction.[12,21,35]

Compounds **7**, **10**, and **11** all contain such a negatively charged dangling chain with a terminal carboxyl group characteristically associated with a high rate of renal excretion in *fac*-$^{99m}Tc^{I}(CO)_3(L)$ agents. Nevertheless, $^{99m}Tc^{I}(CO)_3(NDAP)$ and $^{99m}Tc^{I}(CO)_3(NDPA)$, the respective *fac*-$^{99m}Tc^{I}(CO)_3(L)$ analogues of **10** and **11**, exhibited a significantly reduced rate of renal excretion compared to $^{99m}Tc^{I}(CO)_3(NTA)$.[37] For example, urine activities (as % of that of ^{131}I-OIH, which was used as an internal control) at 10

DOI: 10.1021/acs.inorgchem.5b00584
Inorg. Chem. 2015, 54, 6281−6290

min were 77% for $^{99m}Tc^{I}(CO)_3$(NDAP) and 64% for $^{99m}Tc^{I}(CO)_3$(NDPA), versus 108% for $^{99m}Tc^{I}(CO)_3$(NTA).[37] It may well be that electron donation from the dangling group into the $[^{99m}Tc^{I}(CO)_3(N(CH_2CO_2)_2)]^-$ moiety, as indicated clearly by ^{13}C NMR data for **10**, more than offsets the effect of the negative carboxyl-bearing dangling group. (The ^{13}C NMR shifts of the 5-membered ring CH_2 signal of **10** and **11** are, respectively, ∼1 and 2 ppm further upfield than the relatively similar shifts for this signal in the spectra of **7**, **8**, and **9**.) Alternatively or possibly in combination with the electron-donating inductive effect on ZONE 2, the larger size and greater lipophilicity of the 6-membered chelate ring (such as in **11**) and of the dangling groups (such as in **10** and **11**) are responsible for the significant decrease in clearance of *fac*-$^{99m}Tc^{I}(CO)_3$(L) analogues of **10** and **11**.

SUMMARY AND CONCLUSIONS

We have crystallized and structurally characterized for the first time a *fac*-M(CO)$_3$(NTA) complex, NEt$_4$[*fac*-Re(CO)$_3$(NTAH)], along with a number of related complexes with aminopolycarboxylate ligands. In addition, the crystallographically determined structure of NEt$_4$[*fac*-Re(CO)$_3$(NTAH)] provides compelling evidence that the structure of the promising $^{99m}Tc(CO)_3$(NTA) renal tracer currently undergoing evaluation in patients contains the expected symmetrical ONO coordination mode with two adjacent 5-membered chelate rings.

The reaction progress with the NDPAH$_3$ (**5**) and NTPH$_3$ (**6**) ligands reflects the relative difficulty of forming 6-membered chelate rings. [Re(CO)$_3$(NDPA)]$^{2-}$ (**11**) formed more slowly than complexes **7**−**10**, which have exclusively 5-membered rings. Furthermore, the attempt to make [Re(CO)$_3$(NTP)]$^{2-}$ by using **6**, a ligand which can form only six-membered chelate rings, was not successful (Scheme 1), even after prolonged heating, a result exactly analogous to that obtained in ^{99m}Tc labeling studies with **6**.[37] At physiologically relevant pH, neither **7** nor **11** decomposed detectably, nor did they undergo ligand exchange; thus, ONO coordination with two 5-membered chelate rings or one 5- and one 6-membered chelate ring provides sufficient robustness. The decomposition of **11** in acidic solution is attributed to a facile opening of its 6-membered chelate ring. In highly basic solution, **11** decomposed more slowly than **7**, a result suggesting that deprotonation of a CH in a 5-membered chelate ring initiates decomposition.

The structural details and NMR data we report for complexes **7**, **8**, and **9** indicate that the structural features and the electronic properties of the solvent-exposed atoms in the $[Re(CO)_3(N(CH_2CO_2)_2)]^-$ moiety and projecting away from the dangling chain are very similar, despite the fact that the dangling groups in **7**, **8**, and **9** ($CH_2CO_2^-$, CH_2CONH_2, and CH_2CH_2OH, respectively) differ in charge and other ways. In turn, these findings very strongly indicate that the similar pharmacokinetic properties reported for the ^{99m}Tc analogues of **7**, **8**, and **9**, $^{99m}Tc^{I}(CO)_3$(NTA), $^{99m}Tc^{I}(CO)_3$(ADA), and $^{99m}Tc^{I}(CO)_3$(HDA), all with dangling groups of comparable size, are determined primarily by the features of the solvent-exposed atoms of the $[^{99m}Tc(CO)_3(N(CH_2CO_2)_2)]^-$ moiety itself, rather than by the charge of the dangling group or the presence of a carboxyl group in the dangling chain. This conclusion is also in agreement with our previous results with the $^{99m}Tc(CO)_3$(UEDDA) agent [UEDDAH$_2$ = unsymmetrical ethylenediamine-*N*,*N*-diacetic acid, a ligand with two $CH_2CO_2^-$ chains on one ethylenediamine nitrogen]. At physiological pH, $^{99m}Tc(CO)_3$(UEDDA) has a dangling chain with an uncoordinated carboxyl group but an NNO donor set rather than the ONO iminodiacetate moiety. Hepatobiliary excretion and intestinal secretion of $^{99m}Tc(CO)_3$(UEDDA) were higher compared to the mononegative ^{99m}Tc agents, $^{99m}Tc(CO)_3$(ADA) and $^{99m}Tc(CO)_3$(HDA), both of which have no uncoordinated carboxyl groups.[32,37]

Our interpretation that the inner-sphere ligand properties can dominate over the dangling chain properties is a departure from concepts developed in investigations employing the Re/^{99m}Tc strategy to develop *fac*-$[^{99m}Tc^{I}(CO)_3L]^{n-}$ and $^{99m}Tc^{V}O(L)$ agents reported over several decades. The information gained here into the effects of the dangling group on the structural and electronic properties of the $[^{99m}Tc(CO)_3(N(CH_2CO_2)_2)]^-$ moiety from the study of *fac*-$[Re(CO)_3(L)]^{n-}$ complexes provides a new perspective on the potential roles of the inner-sphere chelate ring atoms and of the dangling chain.

ASSOCIATED CONTENT

Supporting Information

Additional experimental details for complexes **7**−**11**, including yields, ^1H NMR spectral data, and HRMS data; additional details of the NMR signal assignments for **11**; tables of ^1H and ^{13}C NMR shifts of complexes **7**−**11** in D_2O at high and low pH and 25 °C; ^1H NMR spectra of **7**, **10**, and **11**, showing *exo*- and *endo*-CH signals of the 5-membered chelate rings and the N−CH_2 signals of the dangling chain; ROESY spectrum of **7** at pH ∼2.5 in D_2O at 25 °C; ^1H NMR spectra of **11** in D_2O at 25 °C, showing decomposition under acidic conditions; and figure showing the time dependence for the formation of products by ligands **1**−**5**; and CIF files detailing the crystal structures for **7**−**10**. The Supporting Information is available free of charge on the ACS Publications website at DOI: 10.1021/acs.inorgchem.5b00584.

AUTHOR INFORMATION

Corresponding Authors

*(J.K.) Tel: +1-678-360-0352. E-mail: jeff.klenc@gmail.com.
*(L.G.M.) Tel: +1-225-578-0933. E-mail: lmarzil@lsu.edu.

Notes

The authors declare no competing financial interest.

ACKNOWLEDGMENTS

This work was supported by the National Institutes of Health/National Institute of Diabetes and Digestive and Kidney Diseases (Grant No. R37 DK038842). We thank Drs. John Bacsa and Kenneth Hardcastle at Emory for discussions regarding crystal preparation and X-ray structure determination. We also thank Dr. Svetlana Pakhomova at Louisiana State University for final refinements of the molecular structures and for preparing tables, files, and figures of **7**, **8**, **9**, and **10**. L.G.M. thanks the Raymond F. Schinazi International Exchange Programme between the University of Bath, U.K., and Emory University, Atlanta, GA, U.S.A. for a Faculty Fellowship. We also thank Dr. Patricia A. Marzilli for her invaluable comments during the preparation of the manuscript.

DOI: 10.1021/acs.inorgchem.5b00584
Inorg. Chem. 2015, 54, 6281−6290

REFERENCES

(1) Taylor, A.; Schuster, D.; Alazraki, N. In *A Clinician's Guide to Nuclear Medicine*; Society of Nuclear Medicine: Reston, VA, 2006; pp 45−74.
(2) Tubis, M.; Posnick, E.; Nordyke, R. A. *Exp. Biol. Med.* **1960**, *103*, 497−498.
(3) Burbank, M.; Tauxe, W.; Maher, F.; Hunt, J. *Proc. Staff Meet. Mayo Clin.* **1961**, *36*, 372−386.
(4) Eshima, D.; Taylor, A., Jr. *Semin. Nucl. Med.* **1992**, *22*, 61−73.
(5) Shattuck, L.; Eshima, D.; Taylor, A. T.; Anderson, T. L.; Graham, D. L.; Latino, F. A.; Payne, S. E. *J. Nucl. Med.* **1994**, *35*, 349−355.
(6) Sanchez, J.; Freidman, S.; Kempf, J.; Abdel-Dayem, H. *Clin. Nucl. Med.* **1993**, *18*, 30−34.
(7) Rosen, J. *Clin. Nucl. Med.* **1993**, *18*, 713−714.
(8) Taylor, A., Jr.; Eshima, D.; Christian, P.; Wotten, W.; Hansen, L.; McElvany, K. *J. Nucl. Med.* **1988**, *29*, 616−622.
(9) Hansen, L.; Taylor, A. T.; Marzilli, L. G. *Met.-Based Drugs* **1995**, *2*, 105−110.
(10) Lipowska, M.; Hayes, B. L.; Hansen, L.; Taylor, A.; Marzilli, L. G. *Inorg. Chem.* **1996**, *35*, 4227−4231.
(11) Taylor, A.; Hansen, L.; Eshima, D.; Malveaux, E.; Folks, R.; Shattuck, L.; Lipowska, M.; Marzilli, L. G. *J. Nucl. Med.* **1997**, *38*, 821−826.
(12) Taylor, A. T.; Lipowska, M.; Hansen, L.; Malveaux, E.; Marzilli, L. G. *J. Nucl. Med.* **2004**, *45*, 885−891.
(13) Hansen, L.; Marzilli, L. G.; Eshima, D.; Malveaux, E. J.; Folks, R.; Taylor, A., Jr. *J. Nucl. Med.* **1994**, *35*, 1198−205.
(14) Hansen, L.; Cini, R.; Taylor, A.; Marzilli, L. G. *Inorg. Chem.* **1992**, *31*, 2801−2808.
(15) Marzilli, L. G.; Banaszczyk, M. G.; Hansen, L.; Kuklenyik, Z.; Cini, R.; Taylor, A., Jr. *Inorg. Chem.* **1994**, *33*, 4850−4860.
(16) Hansen, L.; Lipowska, M.; Meléndez, E.; Xu, X.; Hirota, S.; Taylor, A. T.; Marzilli, L. G. *Inorg. Chem.* **1999**, *38*, 5351−5358.
(17) Hansen, L.; Hirota, S.; Xu, X.; Taylor, A. T.; Marzilli, L. G. *Inorg. Chem.* **2000**, *39*, 5731−5740.
(18) Lipowska, M.; Hansen, L.; Xu, X.; Marzilli, P. A.; Taylor, A.; Marzilli, L. G. *Inorg. Chem.* **2002**, *41*, 3032−3041.
(19) Lipowska, M.; Hansen, L.; Marzilli, L. G.; Taylor, A. T. *J. Nucl. Med.* **2001**, *42*, S259.
(20) He, H.; Lipowska, M.; Christoforou, A. M.; Marzilli, L. G.; Taylor, A. T. *Nucl. Med. Biol.* **2007**, *34*, 709−716.
(21) Nosco, D. L.; Beaty-Nosco, J. A. *Coord. Chem. Rev.* **1999**, *184*, 91−123.
(22) Lipowksa, M.; Marzilli, L. G.; Taylor, A. T. *J. Nucl. Med.* **2009**, *50*, 454−460.
(23) Lipowska, M.; Klenc, J.; Marzilli, L. G.; Taylor, A. T. *J. Nucl. Med.* **2012**, *53*, 1277−1283.
(24) Banerjee, S. R.; Maresca, K. P.; Francesconi, L.; Valliant, J.; Babich, J. W.; Zubieta, J. *Nucl. Med. Biol.* **2005**, *32*, 1−20.
(25) Schibli, R.; Schubiger, A. P. *Eur. J. Nucl. Med.* **2002**, *29*, 1529−1542.
(26) Alberto, R.; Schibli, R.; Waibel, R.; Abram, U.; Schubiger, A. P. *Coord. Chem. Rev.* **1999**, *190−192*, 901−919.
(27) Alberto, R.; Schibli, R.; Egli, A.; Schubiger, A. P.; Abram, U.; Kaden, T. A. *J. Am. Chem. Soc.* **1998**, *120*, 7987−7988.
(28) Schibli, R.; La Bella, R.; Alberto, R.; Garcia-Garayoa, E.; Ortner, K.; Abram, U.; Schubiger, P. A. *Bioconjugate Chem.* **2000**, *11*, 345−351.
(29) Shen, Y.; Schottelius, M.; Zelenka, K.; De Simone, M.; Pohle, K.; Kessler, H.; Wester, H.-J.; Schmutz, P.; Alberto, R. *Bioconjugate Chem.* **2012**, *24*, 26−35.
(30) Alberto, R.; Bugaj, J. E.; Dyszlewski, M. WO 2001/000637A1, Jan 4, 2001.
(31) Klenc, J.; Lipowska, M.; Taylor, A. T.; Marzilli, L. G. *Eur. J. Inorg. Chem.* **2012**, *2012*, 4334−4341.
(32) Lipowska, M.; He, H.; Xu, X.; Taylor, A. T.; Marzilli, P. A.; Marzilli, L. G. *Inorg. Chem.* **2010**, *49*, 3141−3151.
(33) Taylor, A. T.; Lipowska, M.; Cai, H. *J. Nucl. Med.* **2013**, *54*, 578−584.
(34) Taylor, A. T.; Lipowska, M.; Marzilli, L. G. *J. Nucl. Med.* **2010**, *51*, 391−396.
(35) Shikano, N.; Kanai, Y.; Kawai, K.; Ishikawa, N.; Endou, H. *J. Nucl. Med.* **2004**, *45*, 80−85.
(36) Lipowska, M.; Klenc, J.; Taylor, A. *J. Nucl. Med.* **2014**, *55*, S1206.
(37) Lipowska, M.; Taylor, A. T.; Marzilli, L. G. In *Technetium and Other Radiometals in Chemistry and Medicine*; Mazzi, U., Eckelman, W. C., Volkert, W. A., Eds.; SGEd.iali: Padova, Italy, 2010; pp 281−284.
(38) Murugesu, M.; Clérac, R.; Pilawa, B.; Mandel, A.; Anson, C. E.; Powell, A. K. *Inorg. Chim. Acta* **2002**, *337*, 328−336.
(39) He, H.; Lipowska, M.; Xu, X.; Taylor, A. T.; Carlone, M.; Marzilli, L. G. *Inorg. Chem.* **2005**, *44*, 5437−5446.
(40) *Bruker APEX2*, 6.45A; Bruker AXS Inc.: Madison, WI, 2007.
(41) Sheldrick, G. M. *Acta Crystallogr., Sect. A* **2008**, *64*, 112−122.
(42) Wilson, A. J. C. *International Tables for X-ray Crystallography*; Academic Publishers: Dordrecht, The Netherlands, 1992; Vol. C.
(43) Farrugia, L. *J. Appl. Crystallogr.* **1997**, *30*, 565.
(44) Alberto, R.; Ortner, K.; Wheatley, N.; Schibli, R.; Schubiger, A. P. *J. Am. Chem. Soc.* **2001**, *123*, 3135−3136.
(45) Chaberek, S.; Martell, A. E. *J. Am. Chem. Soc.* **1953**, *75*, 2888−2892.
(46) Mederos, A.; Domínguez, S.; Medina, A. M.; Brito, F.; Chinea, E.; Bazdikian, K. *Polyhedron* **1987**, *6*, 1365−1373.
(47) Araujo, M. L.; Brito, F.; Cecarello, I.; Guilarte, C.; Martinez, J. D.; Monsalve, G.; Oliveri, V.; Rodriguez, I.; Salazar, A. *J. Coord. Chem.* **2008**, *62*, 75−81.
(48) Lipowska, M.; Taylor, A.; Marzilli, L. G. *Nucl. Med. Biol.* **2010**, *37*, 697−698.
(49) Marti, N.; Spingler, B.; Breher, F.; Schibli, R. *Inorg. Chem.* **2005**, *44*, 6082−6091.
(50) Britten, J. F.; Lock, C. J. L.; Pratt, W. M. C. *Acta Crystallogr., Sect. B* **1982**, *38*, 2148−2155.
(51) Maheshwari, V.; Carlone, M.; Fronczek, F. R.; Marzilli, L. G. *Acta Crystallogr., Sect. B* **2007**, *63*, 603−611.
(52) Christoforou, A. M.; Marzilli, P. A.; Fronczek, F. R.; Marzilli, L. G. *Inorg. Chem.* **2007**, *46*, 11173−11182.
(53) Perera, T.; Marzilli, P. A.; Fronczek, F. R.; Marzilli, L. G. *Inorg. Chem.* **2010**, *49*, 2123−2131.
(54) Lipowska, M.; Cini, R.; Tamasi, G.; Xu, X.; Taylor, A. T.; Marzilli, L. G. *Inorg. Chem.* **2004**, *43*, 7774−7783.
(55) He, H.; Lipowska, M.; Xu, X.; Taylor, A. T.; Marzilli, L. G. *Inorg. Chem.* **2007**, *46*, 3385−3394.
(56) Perera, T.; Marzilli, P. A.; Fronczek, F. R.; Marzilli, L. G. *Inorg. Chem.* **2010**, *49*, 5560−5572.
(57) Buckingham, D. A.; Marzilli, L. G.; Sargeson, A. M. *J. Am. Chem. Soc.* **1967**, *89*, 3428−3433.

DOI: 10.1021/acs.inorgchem.5b00584
Inorg. Chem. 2015, 54, 6281−6290